

Video Article

Oral Biofilm Formation on Different Materials for Dental Implants

Thalisson S. O. Silva¹, Alice R. Freitas¹, Marília L. L. Pinheiro¹, Cássio do Nascimento¹, Evandro Watanabe², Rubens F. Albuquerque¹

¹Department of Dental Materials and Prosthodontics, School of Dentistry of Ribeirão Preto, University of São Paulo

²Department of Restorative Dentistry, School of Dentistry of Ribeirão Preto, University of São Paulo

Correspondence to: Rubens F. Albuquerque at rubens.albuquerque@usp.br

URL: <https://www.jove.com/video/57756>

DOI: [doi:10.3791/57756](https://doi.org/10.3791/57756)

Keywords: Medicine, Issue 136, Microbiology, biofilms, bacteria, microbial viability, microscopy, multiphoton, scanning electron microscopy, energy dispersive X-ray spectroscopy, clinical assessment, dental materials, zirconia, titanium

Date Published: 6/24/2018

Citation: Silva, T.S., Freitas, A.R., Pinheiro, M.L., do Nascimento, C., Watanabe, E., Albuquerque, R.F. Oral Biofilm Formation on Different Materials for Dental Implants. *J. Vis. Exp.* (136), e57756, doi:10.3791/57756 (2018).

Abstract

Dental implants and their prosthetic components are prone to bacterial colonization and biofilm formation. The use of materials that provides low microbial adhesion may reduce the prevalence and progression of peri-implant diseases. In view of the oral environment complexity and oral biofilm heterogeneity, microscopy techniques are needed that can enable a biofilm analysis of the surfaces of teeth and dental materials. This article describes a series of protocols implemented for comparing oral biofilm formation on titanium and ceramic materials for prosthetic abutments, as well as the methods involved in oral biofilms analyses at the morphological and cellular levels. The *in situ* model to evaluate oral biofilm formation on titanium and zirconia materials for dental prosthesis abutments as described in this study provides a satisfactory preservation of the 48 h biofilm, thereby demonstrating methodological adequacy. Multiphoton microscopy allows the analysis of an area representative of the biofilm formed on the test materials. In addition, the use of fluorophores and the processing of the images using multiphoton microscopy allows the analysis of the bacterial viability in a very heterogeneous population of microorganisms. The preparation of biological specimens for electron microscopy promotes the structural preservation of biofilm, images with good resolution, and no artifacts.

Video Link

The video component of this article can be found at <https://www.jove.com/video/57756/>

Introduction

Bacterial biofilms are complex, functionally and structurally organized microbial communities, characterized by a diversity of microbial species that synthesize an extracellular, biologically active polymer matrix^{1,2}. The bacterial adhesion to biotic or abiotic surfaces is preceded by a formation of the acquired pellicle, mainly consisting of salivary glycoproteins^{1,3,4}. Weak physicochemical interactions between the microorganisms and the pellicle are initially established and followed by stronger interactions between bacterial adhesins and glycoprotein receptors of the acquired pellicle. Microbial diversity gradually increases through the coaggregation of secondary colonizers to the receptors of the already attached bacteria, forming a multispecies community^{1,3,4,5}.

Homeostasis of the oral microbiota and its symbiotic relationship with the host is important in maintaining oral health. The dysbiosis within oral biofilms may increase the risk for the development of caries and periodontal disease^{2,5}. Clinical studies demonstrate a cause-and-effect relationship between the accumulation of biofilm on teeth or dental implants and the development of gingivitis or peri-implant mucositis^{6,7}. The progression of the inflammatory process leads to peri-implantitis and the consequent loss of the implant⁸.

Dental implants and their prosthetic components are prone to bacterial colonization and biofilm formation⁹. The use of materials with a chemical composition and surface topography that provides low microbial adhesion may reduce the prevalence and progression of peri-implant diseases^{9,10}. Titanium is the most-used material for the manufacture of prosthetic abutments for implants; however, ceramic materials were recently introduced and are gaining popularity as an alternative to titanium because of their aesthetic properties and biocompatibility^{11,12}. Also importantly, ceramic materials have been associated with a supposedly reduced potential to adhere to microorganisms, mainly due to their surface roughness, wettability, and surface free energy^{10,13}.

In vitro studies have contributed to significant advances in the understanding of microbial adhesion to prosthetic abutment surfaces^{9,14,15,16,17}. However, the dynamic environment of the oral cavity, characterized by its varying temperature and pH and nutrient availability, as well as by the presence of shear forces, is not reproducible in *in vitro* experimental protocols^{18,19}. To overcome this problem, an alternative is the use of *in situ* models of biofilm formation, which advantageously preserves its three-dimensional structure for *ex vivo* analysis^{10,20,21,22,23,24}.

The analysis of the complex structure of the biofilm formed on oral substrates requires the use of microscopy techniques capable of displaying optically dense matter²⁵. Multiphoton laser scanning microscopy is a modern option for biofilm structural analysis²⁶. It is characterized by the use of nonlinear optics with an illumination source close to the infrared wavelength, pulsed to femtoseconds²⁷. This method is indicated for the image acquisition of autofluorescence materials or materials marked by fluorophores, in addition to images generated by non-linear optical signals

derived from a phenomenon known as Second Harmonic Generation. Among the advantages of multiphoton microscopy is the great image depth obtained with minimum cell damage caused by the intensity of the excitation light²⁷.

For a viability analysis of biofilm on abiotic surfaces by multiphoton microscopy, the use of fluorescent nucleic acid dyes with different spectral characteristics and a penetration capacity in bacterial cells is required²⁸. Fluorophores SYTO9 (green-fluorescent) and propidium iodide (red-fluorescent) can be used for a visual differentiation between live and dead bacteria^{28,29,30}. Propidium iodide penetrates only bacteria with damaged membranes, while SYTO9 enters bacterial cells with an intact and compromised membrane. When both dyes are present inside a cell, propidium iodide has a greater affinity for nucleic acids and displaces SYTO9, marking it red^{28,30}.

In view of the oral environment complexity and oral biofilm heterogeneity, microscopy techniques are needed that can enable the biofilm analysis of the surfaces of teeth and dental materials. This article describes a series of protocols implemented for comparing oral biofilm formation on titanium and ceramic materials for prosthetic abutments, as well as the methods involved in oral biofilms analyses at the morphological and cellular levels.

Protocol

This study was approved by the Institutional Review Board of the School of Dentistry of Ribeirão Preto, and the volunteer participant signed the written consent (Process 2011.1.371.583).

1. Biofilm Formation *in Situ*

1. Selection of participants

1. Select patients based on the following inclusion criteria: a healthy individual with a complete dentition and no clinical signs of oral diseases.
2. Exclude patients based on the following exclusion criteria: pregnancy, lactation, dental caries, a periodontal disease or antibiotic treatment in the last 3 months, smoker, or any systemic disease that could influence the periodontal status.

2. Preparation of intraoral device

1. Record the maxillary arch by means of an alginate impression.
2. Prepare type IV stone by adding 19 mL of water to 100 g of stone powder. Pour the stone into the alginate mold to make a model of the maxillary arch.
3. Design and fabricate an acrylic intraoral device to support the test specimens (titanium and ceramic disks).
 1. Fabricate retentive clasps from NiCr wire (0.7 mm in diameter) using orthodontic pliers #139 and position them on the model. To position the clamp between the upper premolars, bend one end of each wire so that they form a loop.
 1. Adapt the loop in the region of the interdental papilla. In the occlusal, insert a gentle curvature so as not to interfere with the points of contact and with the occlusion. Make a 90° fold at the end of the clamp for a retention in the acrylic.
 2. To fit the clamp in the upper second molar, adapt the curvature of the wire in the cervical third (vestibular) to contour the tooth (distal) and make a 90° fold at the end of the clamp for a retention in the acrylic.

NOTE: In order to provide adequate retention/stability to the intraoral device, the retentive clasps were positioned between the upper premolars and distal aspect of the second molar on both sides of the dental arch.
2. Manipulate the self-curing acrylic resin according to the manufacturer's instructions and press the acrylic resin between 2 glass plates (with a 3 mm thick spacer interposed) during the plastic phase, to make a 3 mm thick sheet.
3. Lay the acrylic sheet on the palatal region of the model, according to the device's design, and trim off the surplus acrylic resin with a carver, before polymerization.
4. Fabricate wax disks using a metallic matrix [10 mm in diameter, 2 mm in thickness (surface area of 78.5 mm²)] by placing molten wax in the matrix and waiting for the wax to solidify. Manually embed 4 wax disks into the acrylic resin, 2 of them between the premolars and the other 2 next to the second molars.
5. Let the acrylic resin polymerize in a pressure pot under 20 psi of compressed air for 20 min.
6. Finish the intraoral device with an electric dental lab handpiece and cutter and polish it with abrasive rubber.
7. Adjust the device for a proper fit in the mouth using the equipment described above.

3. Preparation of the titanium and zirconia specimens

Note: Specimens ($n = 14$) are 10 mm in diameter and 2 mm in thickness and have a surface area of 78.5 mm².

1. Polish the specimens' surfaces with water-cooled sandpapers of decreasing abrasiveness (600, 1200, and 2000 grit), for approximately 20 min.

NOTE: The polishing of the specimens was performed to standardize the surface roughness at 0.2 μm .
2. Clean and disinfect the specimens and intraoral device with liquid detergent and tap water, and then use an isopropyl alcohol ultrasonic bath for 15 min. Dry them with absorbent paper towels.
3. Fix the specimens in the intraoral oral device with about 0.1 mL of non-toxic hot melt adhesive (**Figure 1**).
4. Install the device containing the specimens in the oral cavity.

NOTE: The intraoral device containing the specimens should be worn for 48 h. The device was removed and stored in phosphate buffered saline (PBS) while the patient was eating and performing oral cleaning.

2. Assessment of Bacterial Viability

Note: The sample size $n = 10$.

1. Prepare a dyeing solution by adding 3 μL of SYTO9 (green fluorescent nucleic acid dye) and 3 μL of propidium iodide (red fluorescent nucleic acid dye) to 1 mL of sterile distilled water.
NOTE: Prepare solutions protected from light.
2. Transfer the specimens to a 24-well plate and wash them thoroughly with PBS to remove any non-adherent cells.
3. Add the appropriate volume (1 mL) of fluorescent dye solution to cover the biofilm-containing specimen. Add the dye very carefully so as not to disorganize the biofilm.
4. Incubate the specimen for 20 - 30 min at room temperature, protected from light.
5. Gently wash the biofilm sample with sterile distilled water to remove any excess dye.
6. Place the specimen in a glass bottom dish and perform multiphoton laser scanning microscopy for the biofilm analysis.
NOTE: The analysis of the bacterial cells viability was carried out using a multiphoton microscopy system. The fluorescence of propidium iodide was detected using a filter with an excitation/emission wavelength of 546/680 nm and 477/600 nm for SYTO9. The size of the images obtained was 5.16188 x 5.16188 mm, which corresponds to 26.64 mm² of the total area of each specimen (78.5 mm²) or 33.94% of the total area. The images were made from the most central portion of the sample, with a resolution of 1,024 x 1,024 pixels. The red channel and green channel images were analyzed separately using Fiji software³¹. Each cell was selected using a selection tool and the intensity of the fluorescence was measured through the integrated density of the pixels, subtracting the image background.

3. Analysis of the Specimens' Chemical Composition by Energy Dispersive Spectroscopy (EDS)

Note: The sample size $n = 3$.

1. Select 3 specimens of each biofilm-free test material, and assess the chemical composition in 2 different areas of each specimen using a scanning electron microscope coupled to a dispersive energy spectrometer, with an electron beam voltage of 10 kV³².

4. Morphological Analysis of the Bacterial Biofilm by Scanning Electron Microscopy

Note: The sample size $n = 1$.

1. Fix the biofilm by immersing the specimens in 2.5% glutaraldehyde diluted in 0.1 M sodium cacodylate buffer, pH 7.0 - 7.3, for 24 h.
2. Wash the sample in PBS buffer (pH = 7.6).
3. Postfix the biofilm with 1% osmium tetroxide for 1 h.
4. Wash the sample in PBS buffer (pH = 7.6).
5. Dehydrate the biofilm samples carefully, keeping them immersed in increasing concentrations of ethanol solutions (50%, 70%, 90%, 95%, and 100%).
NOTE: Perform 3 exchanges of ethanol at a 100% concentration. The total dehydration step takes about 2 h.
6. Transfer the specimens to the critical point dryer and make several substitutions with carbon dioxide (CO₂) until the specimens are dry.
7. Remove the dried specimens from the apparatus and mount them onto the scanning electron microscope holders.
8. Sputter-coat a 20 nm layer of gold onto the specimen's surface for 120 s.
9. Insert the gold-coated discs in the scanning electron microscope chamber. Obtain images from 5 different areas of each specimen, at 20 - 30 kV under variable pressure and at 650X magnification¹².

Representative Results

The colonization density of the biofilm after 48 h of *in situ* growth was represented in this study by the proportion of the colonized area on the titanium and zirconia disks in relation to the total scanned area of the specimen using multiphoton microscopy (26.64 mm²). **Figure 2** represents the bacterial colonization density on the surface of the 3 tested materials. A higher density of biofilm was observed on the surfaces of the cast and on the machined titanium disks (0.0292 μm^2 and 0.0213 μm^2 , respectively) than in the zirconia disks (0.0099 μm^2 ; $p < 0.05$; Kruskal-Wallis test, followed by Dunn's test).

Figure 3 shows the bacterial cells viability on the surfaces of zirconia (**Figure 3A**, **3A'**, and **3A''**), machined titanium (**Figure 3B**, **3B'**, and **3B''**), and cast titanium (**Figure 3C**, **3C'**, and **3C''**) disks. In this protocol, the nucleic acid dye propidium iodide penetrates only into bacteria with a damaged membrane and, therefore, emits a red-fluorescent signal that is related to dead cells. SYTO9 penetrates the bacterial cells with intact or compromised membrane and emits a green fluorescent signal from live microorganisms. Cellular bacterial viability was similar between the test materials, with a predominance of live microorganisms in all groups (**Figure 4**). Live/dead cells proportions were 2.10 for zirconia, 1.95 for machined titanium, and 1.63 for cast titanium.

Cracks, grooves, or abrasion defects produced on the surface of all materials during the process of polishing and/or machining were observed, more clearly in machined and cast titanium disks. In the zirconia disks, larger areas were observed with an absence of microorganisms; small polymorphic microbial aggregates consisting mainly of cocci, bacilli, and filamentous bacteria were also observed (**Figure 5A** and **5A'**). The presence of cocci and bacilli was scattered on the surfaces of machined titanium disks (**Figure 5B** and **5B'**). Cast titanium specimens presented colonies of microorganisms involved in a matrix with a biofilm-like appearance on the surface (**Figure 5C** and **5C'**). Less matrix material was observed on the surface of the zirconia disks compared to the machined titanium and cast titanium disks.

The EDS analysis revealed 70.83% of zirconia, 22.84% of oxygen, 4.52% of yttrium, and 1.57% of hafnium in the zirconia disks; 95.16% of titanium, 3.99% of oxygen, and 0.85% of carbon in the cast titanium disks; and 89.86% of titanium, 7.53% of oxygen, and 2.61% of carbon in the machined titanium disks (**Figure 6**).

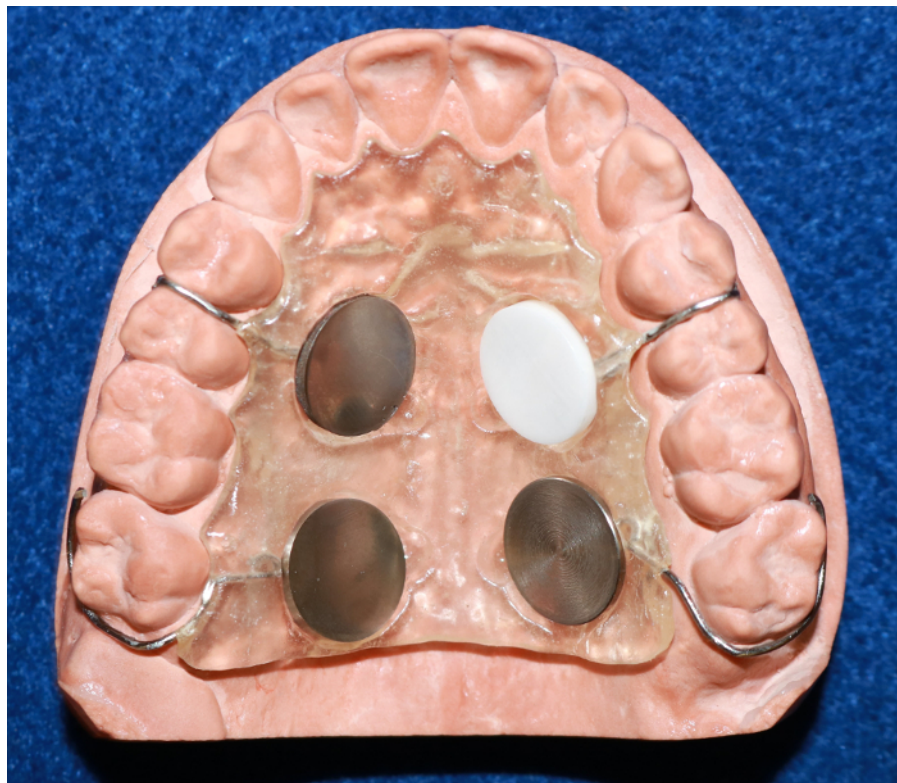


Figure 1: The intraoral device for the *in situ* study. Retentive clasps were fabricated with wrought wire, and titanium and zirconia test disks (10 mm in diameter, 2 mm thick) were randomly positioned in the premolars and molars regions, partially embedded in self-curing acrylic resin. [Please click here to view a larger version of this figure.](#)

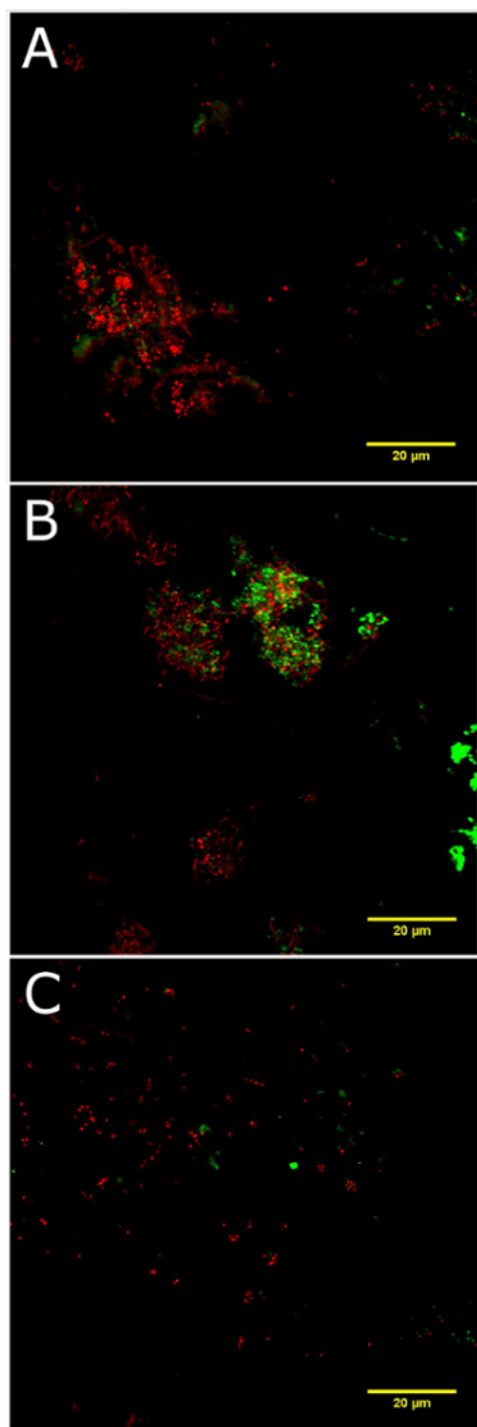


Figure 2: Fluorescence images of the bacterial cell density. These are fluorescence images of the bacterial cell density on (A) zirconia, (B) machined titanium, and (C) cast titanium disks after 48 h *in situ*. [Please click here to view a larger version of this figure.](#)

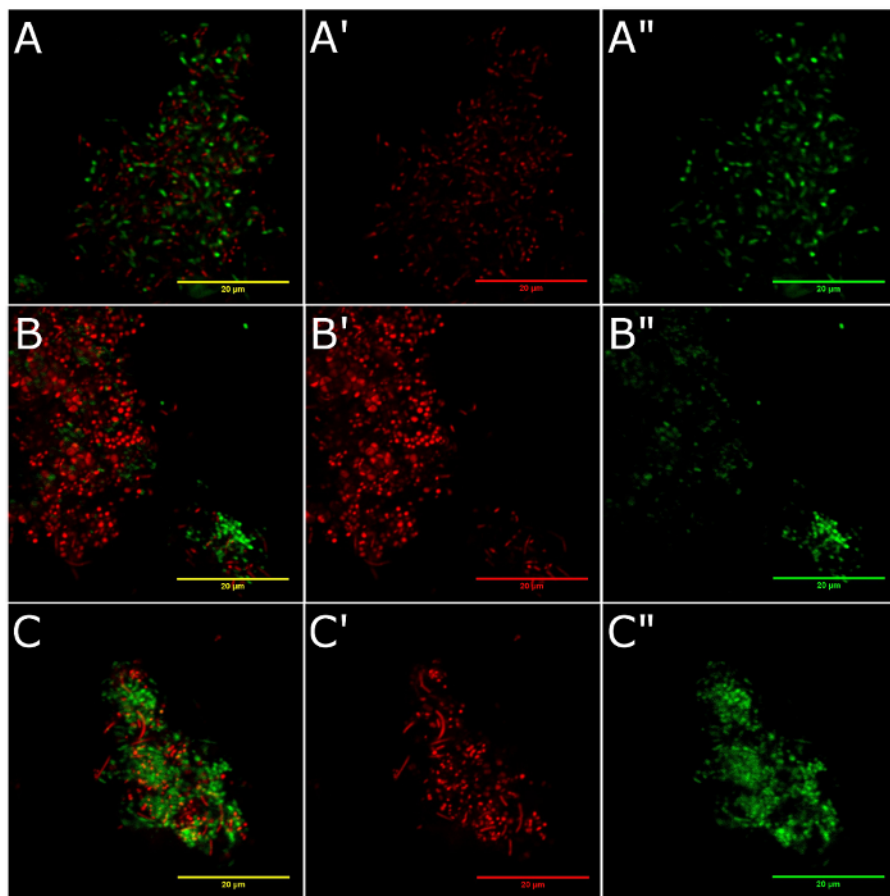


Figure 3: The cell viability of bacteria adhered to the surfaces. These panels show the cell viability of bacteria adhered to the surfaces of (A) dead and live bacterial cells on zirconia, (B) dead and live bacterial cells on machined titanium, and (C) dead and live bacterial cells on cast titanium disks depicted by fluorescence imaging. Dead bacterial cells are stained with propidium iodide (A', B', and C': red-fluorescent signal). Live bacteria are stained with SYTO9 (A'', B'', and C'': green fluorescence signal). Panels A, B, and C show color-merged images. [Please click here to view a larger version of this figure.](#)

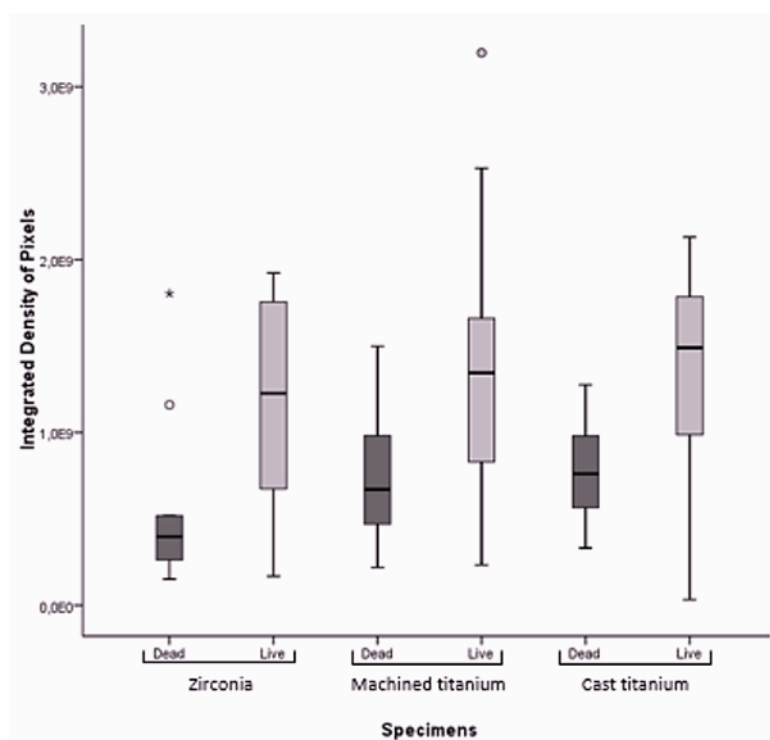


Figure 4: Boxplots representing the biofilm's cell viability on the different test materials. [Please click here to view a larger version of this figure.](#)

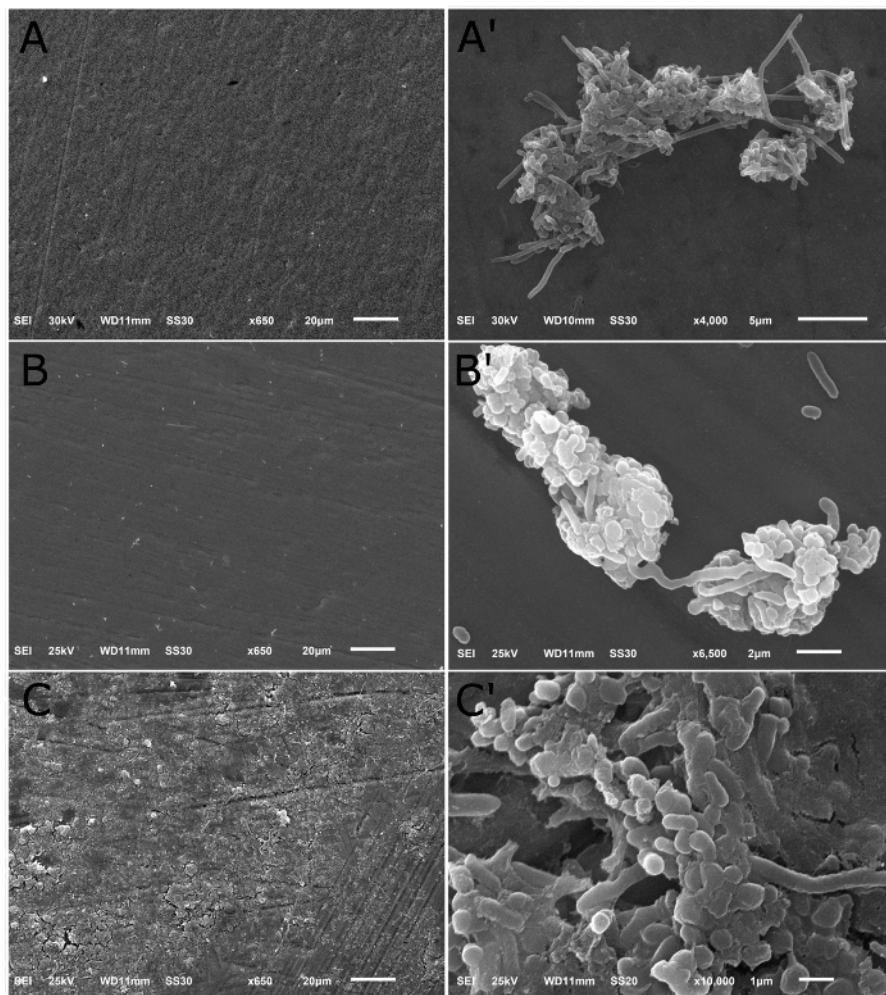


Figure 5: Scanning electron microscopy. These panels show the scanning electron microscopy of (A, A') zirconia, (B, B') machined titanium, and (C, C') cast titanium disks with biofilm, in panoramic and close up views, after 48 h *in situ*. [Please click here to view a larger version of this figure.](#)

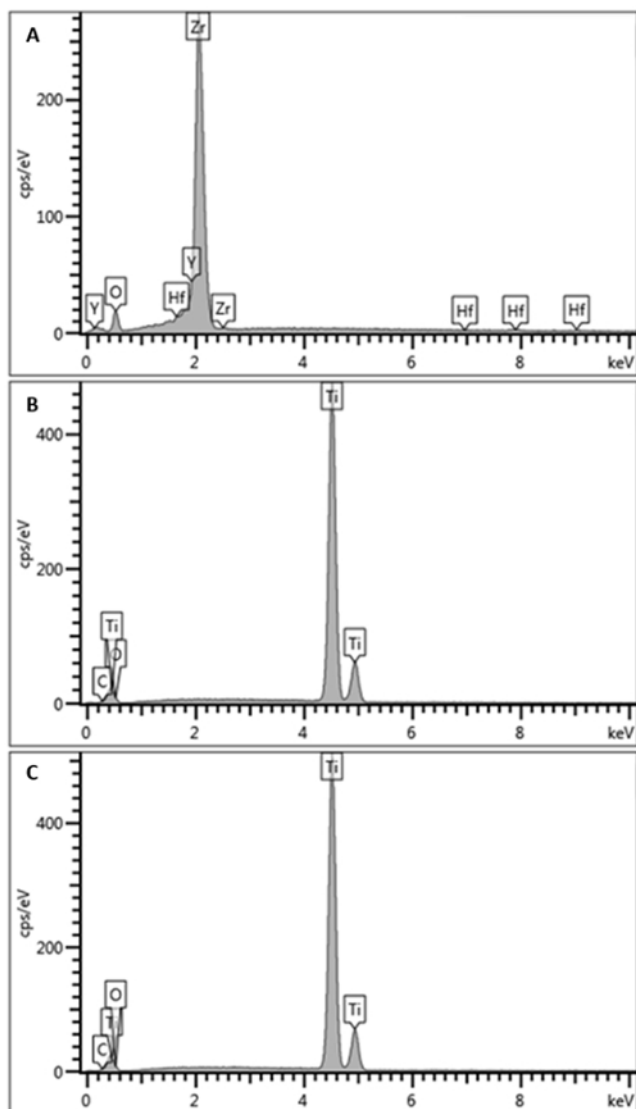


Figure 6: An elemental analysis by Energy Dispersive Spectroscopy (EDS). These panels show (A) zirconsia disks (Zr = zirconsia, Y = yttrium, C = carbon, O = oxygen, and Hf = hafnium); (B) machined titanium, and (C) cast titanium disks (Ti = titanium, O = oxygen, and C = carbon). [Please click here to view a larger version of this figure.](#)

Discussion

The protocol described in this study was developed to evaluate the biofilm formation on titanium and zirconsia materials for prosthetic abutments, including the analysis of bacterial cell viability and morphological characteristics. In order to accomplish this, an *in situ* model of biofilm formation was designed, consisting of an intraoral device capable to accommodate samples of the test materials and keep them exposed to the dynamic oral environment for 48 h. The device was considered comfortable and easy to insert, remove, and clean by the volunteer. Yet, it showed little impact on phonetics and aesthetics, was simple and low-cost to fabricate, and allowed an easy recovery of the specimens without disruption of the biofilm structure. Moreover, the method allowed the preservation of the bacterial cells and the extracellular matrix's integrity. The contact of the tongue with the specimens and the accidental loss of the disc during the experiment are limitations of the proposed model. In order to minimize the limitations of the method, the positioning of the discs in the intraoral device was randomly distributed; in addition, the discs were fixed with non-toxic hot melt adhesive, and no loss of sample was reported.

Due to the high heterogeneity of the bacterial species inhabiting the oral environment, powerful microscopy techniques are required for the analysis of biofilms colonizing its hard surfaces. Multiphoton microscopy provides several advantages over conventional or confocal microscopy analyses, such as an inherent three-dimensional resolution, a near-infrared excitation for superior optical penetration, a reduction of photobleaching and photodamage when imaging live cells, and a capability to provide quantitative information^{33,34}. These advantages originate through the highly localized excitation of the two-photon absorption process and the reduced effect of light scattering in the specimens. Therefore, multiphoton microscopy enables deep tissue imaging, minimum cell damage, and an initiation of well-localized photochemistry³⁴. Random sampling and a representative number of fields are to be elected for accurate analyses^{35,36}. The multiphoton laser scanning microscopy allowed the analysis of areas of 5161.88 x 5161.88 μm , corresponding to 33.94% of the total specimen's area. Confocal microscopy was not used because of the need for a large number of fields for the representative analysis and a long period of evaluation of the specimens. Moreover,

the out-of-focus background signal limited the use of fluorescence microscopy. Despite the advantages of multiphoton microscopy, only a few applications in the microbiological field are reported^{37,38,39}. Among them is its use as a manipulation tool; for example, to achieve localized ablation, apoptosis/necrosis, bleaching, or photoactivation of a well-defined volume of biofilm cells²⁶. Another application of this method is to evaluate the efficacy of antibacterial agents against multiple biofilm components^{25,40,41}.

In this study, the viability of adhered bacterial cells was evaluated with fluorescent nucleic acid dyes, which penetrate cells as a function of their membrane integrity²⁸. SYTO9 fluorophores and propidium iodide were used for the visual differentiation between live and dead bacteria. Some limitations of the use of SYTO9 and propidium iodide are reported in the literature, such as the difficulty of SYTO9 to stain gram-negative bacteria with an intact membrane because it has to cross the two cell membranes present in the structure^{30,42}. Thus, live cells can be underestimated by a combined staining. In addition, when SYTO9 is not completely replaced by propidium iodide, yellow fluorescence may be observed instead of red in bacterial cells^{30,42}. Another limitation is the decrease of the SYTO9 signal over time. It is recommended that the microscopy analyses are performed within 30 min after the exposure to the dyes^{29,30}. It is necessary to consider the background fluorescence to calculate the signal intensity, since the autofluorescence of the substrate and the presence of unbound dye may interfere with the results³⁰. Nevertheless, since these limitations are well reported, it is possible to have the samples processed within the specified timeframe, as well as to carefully select and subtract the images' background with the aid of the Fiji software.

High vacuum and electron irradiation during scanning electron microscopy represent adverse conditions for samples containing biological material. In addition to non-conductive properties, the biofilm in its natural state is hydrated, which interferes with the electron generation and detection system, forming artifacts⁴³. Therefore, specimens containing biological material must be prepared in order to ensure the preservation of the structure and conduction of their electrons^{43,44}. The protocol phases involving fixation, dehydration, drying, and coating of the specimens with conductive material were developed with particular attention to the dilutions and time. The fixation of the biological material was performed with an aldehyde in a cacodylate buffer and the post-fixation with osmium tetroxide, in order to preserve the structure of the adhered biofilm^{43,45,46}. Dehydration was achieved with an ascending series of ethanol concentrations, with the water being gradually replaced by the organic solvent⁴⁴. Drying with a minimal distortion of the biofilm architecture was performed through the critical point with successive replacements of liquid CO₂ for the ethanol removal, followed by a conversion of CO₂ to gas phase, a removal of the liquid/gas interface, and the elimination of surface tension on the specimen^{43,44,45,46}. To ensure the conductivity of the electrons, prevent or reduce damage, and image the artifacts, the specimens were coated with a 10 - 20 nm layer of gold or gold/palladium. In addition, coating the specimens with a thin layer of metal can reduce the electrical charge build-up within a specimen, improve contrast, and increase image resolution⁴⁶.

Despite some limitations, the *in situ* model described in this study was adequate for the evaluation of oral biofilm formation on titanium and zirconia materials, preserving the 48 h biofilm. The use of fluorophores associated with imaging by multiphoton microscopy allowed the analysis of the bacterial cell viability in a very heterogeneous population of microorganisms colonizing the test materials. The techniques employed in the preparation of the biological samples promoted the biofilm's structural preservation and allowed the acquisition of high-quality images for the visualization and morphological characterization of the colonizing microorganisms.

Disclosures

The authors have nothing to disclose.

Acknowledgements

The authors thank José Augusto Maulin from Microscopy Multiuser Laboratory (School of Medicine of Ribeirão Preto) for his generous assistance with the EDS and SEM analyses and Hermano Teixeira Machado for his generous technical assistance in the video edition.

References

1. Do, T., Devine, D., Marsh, P. D. Oral biofilms: molecular analysis, challenges, and future prospects in dental diagnostics. *Clinical, Cosmetic and Investigational Dentistry*. **5**, 11-19 (2013).
2. Samaranayake, L., Matsubara, V. H. Normal Oral Flora and the Oral Ecosystem. *Dental Clinics of North America*. **61** (2), 199-215 (2017).
3. Larsen, T., Fiehn, N. E. Dental biofilm infections - an update. *Acta Pathologica, Microbiologica, et Immunologica Scandinavica*. **125** (4), 376-384 (2017).
4. Marsh, P. D., Do, T., Beighton, D., Devine, D. A. Influence of saliva on the oral microbiota. *Periodontology 2000*. **70** (1), 80-92 (2016).
5. Marsh, P. D., Zaura, E. Dental biofilm: ecological interactions in health and disease. *Journal of Clinical Periodontology*. **44** Suppl 18, S12-S22 (2017).
6. Zitzmann, N. U., Berglundh, T., Marinello, C. P., Lindhe, J. Experimental peri-implant mucositis in man. *Journal of Clinical Periodontology*. **28** (6), 517-523 (2001).
7. Meyer, S. *et al.* Experimental mucositis and experimental gingivitis in persons aged 70 or over. Clinical and biological responses. *Clinical Oral Implants Research*. **28** (8), 1005-1012 (2017).
8. Salvi, G. E., Cosgarea, R., Sculean, A. Prevalence and Mechanisms of Peri-implant Diseases. *Journal of Dental Research*. **96** (1), 31-37 (2017).
9. Hahnel, S., Wieser, A., Lang, R., Rosentritt, M. Biofilm formation on the surface of modern implant abutment materials. *Clinical Oral Implants Research*. **26** (11), 1297-1301 (2015).
10. Nascimento, C. *et al.* Bacterial adhesion on the titanium and zirconia abutment surfaces. *Clinical Oral Implants Research*. **25** (3), 337-343 (2014).
11. Nakamura, K., Kanno, T., Milleding, P., Ortengren, U. Zirconia as a dental implant abutment material: a systematic review. *The International Journal of Prosthodontics*. **23** (4), 299-309 (2010).

12. Scarano, A., Piattelli, M., Caputi, S., Favero, G. A., Piattelli, A. Bacterial adhesion on commercially pure titanium and zirconium oxide disks: an *in vivo* human study. *Journal of Periodontology*. **75** (2), 292-296 (2004).
13. Nascimben, C. *et al.* Microbiome of titanium and zirconia dental implants abutments. *Dental Materials*. **32** (1), 93-101 (2016).
14. Rimondini, L., Cerroni, L., Carrassi, A., Torricelli, P. Bacterial colonization of zirconia ceramic surfaces: an *in vitro* and *in vivo* study. *The International Journal of Oral & Maxillofacial Implants*. **17** (6), 793-798 (2002).
15. de Avila, E. D., Avila-Campos, M. J., Vergani, C. E., Spolidorio, D. M., Mollo Fde, A., Jr. Structural and quantitative analysis of a mature anaerobic biofilm on different implant abutment surfaces. *Journal of Prosthetic Dentistry*. **115** (4), 428-436 (2016).
16. de Avila, E. D. *et al.* Impact of Physical Chemical Characteristics of Abutment Implant Surfaces on Bacteria Adhesion. *Journal of Oral Implantology*. **42** (2), 153-158 (2016).
17. de Avila, E. D. *et al.* Effect of titanium and zirconia dental implant abutments on a cultivable polymicrobial saliva community. *Journal of Prosthetic Dentistry*. **118** (4), 481-487 (2017).
18. Lin, N. J. Biofilm over teeth and restorations: What do we need to know? *Dental Materials*. **33** (6), 667-680 (2017).
19. Prada-Lopez, I., Quintas, V., Tomas, I. The intraoral device of overlaid disk-holding splints as a new *in situ* oral biofilm model. *Journal of Clinical and Experimental Dentistry*. **7** (1), e126-132 (2015).
20. Prada-Lopez, I., Quintas, V., Vilaboa, C., Suarez-Quintanilla, D., Tomas, I. Devices for *in situ* Development of Non-disturbed Oral Biofilm. A Systematic Review. *Frontiers in Microbiology*. **7**, 1055 (2016).
21. Burgers, R. *et al.* *In vivo* and *in vitro* biofilm formation on two different titanium implant surfaces. *Clinical Oral Implants Research*. **21** (2), 156-164 (2010).
22. do Nascimento, C. *et al.* Oral biofilm formation on the titanium and zirconia substrates. *Microscopy Research and Technique*. **76** (2), 126-132 (2013).
23. Al-Ahmad, A. *et al.* *In vivo* study of the initial bacterial adhesion on different implant materials. *Archives of Oral Biology*. **58** (9), 1139-1147 (2013).
24. Al-Ahmad, A. *et al.* Bacterial adhesion and biofilm formation on yttria-stabilized, tetragonal zirconia and titanium oral implant materials with low surface roughness - an *in situ* study. *Journal of Medical Microbiology*. **65** (7), 596-604 (2016).
25. Thomsen, H. *et al.* Delivery of cyclodextrin polymers to bacterial biofilms - An exploratory study using rhodamine labelled cyclodextrins and multiphoton microscopy. *International Journal of Pharmaceutics*. **531** (2), 650-657 (2017).
26. Lakins, M. A., Marrison, J. L., O'Toole, P. J., van der Woude, M. W. Exploiting advances in imaging technology to study biofilms by applying multiphoton laser scanning microscopy as an imaging and manipulation tool. *Journal of Microscopy*. **235** (2), 128-137 (2009).
27. Zipfel, W. R., Williams, R. M., Webb, W. W. Nonlinear magic: multiphoton microscopy in the biosciences. *Nature Biotechnology*. **21** (11), 1369-1377 (2003).
28. Stocks, S. M. Mechanism and use of the commercially available viability stain, BacLight. *Cytometry Part A*. **61** (2), 189-195 (2004).
29. Johnson, M. B., Criss, A. K. Fluorescence microscopy methods for determining the viability of bacteria in association with mammalian cells. *Journal of Visualized Experiments*. (79), e50729 (2013).
30. Stiefel, P., Schmidt-Emrich, S., Maniura-Weber, K., Ren, Q. Critical aspects of using bacterial cell viability assays with the fluorophores SYTO9 and propidium iodide. *BMC Microbiology*. **15**, 36 (2015).
31. Schindelin, J. *et al.* Fiji: an open-source platform for biological-image analysis. *Nature Methods*. **9** (7), 676-682 (2012).
32. Placko, H. E., Mishra, S., Weimer, J. J., Lucas, L. C. Surface characterization of titanium-based implant materials. *The International Journal of Oral & Maxillofacial Implants*. **15** (3), 355-363 (2000).
33. So, P. T., Dong, C. Y., Masters, B. R., Berland, K. M. Two-photon excitation fluorescence microscopy. *Annual Review of Biomedical Engineering*. **2**, 399-429 (2000).
34. Benninger, R. K., Piston, D. W. Two-photon excitation microscopy for the study of living cells and tissues. *Current Protocols in Cell Biology*. **Chapter 4**, Unit 4. 11. 11-24 (2013).
35. Gardi, J. E., Nyengaard, J. R., Gundersen, H. J. The proportionator: unbiased stereological estimation using biased automatic image analysis and non-uniform probability proportional to size sampling. *Computers in Biology and Medicine*. **38** (3), 313-328 (2008).
36. Melvin, N. R., Poda, D., Sutherland, R. J. A simple and efficient alternative to implementing systematic random sampling in stereological designs without a motorized microscope stage. *Journal of Microscopy*. **228** (Pt 1), 103-106 (2007).
37. Neu, T. R., Kuhlcke, U., Lawrence, J. R. Assessment of fluorochromes for two-photon laser scanning microscopy of biofilms. *Applied and Environmental Microbiology*. **68** (2), 901-909 (2002).
38. Neu, T. R., Woelfl, S., Lawrence, J. R. Three-dimensional differentiation of photo-autotrophic biofilm constituents by multi-channel laser scanning microscopy (single-photon and two-photon excitation). *Journal of Microbiological Methods*. **56** (2), 161-172 (2004).
39. Neu, T. R., Lawrence, J. R. Innovative techniques, sensors, and approaches for imaging biofilms at different scales. *Trends in Microbiology*. **23** (4), 233-242 (2015).
40. Lacroix-Gueu, P., Briandet, R., Leveque-Fort, S., Bellon-Fontaine, M. N., Fontaine-Aupart, M. P. *In situ* measurements of viral particles diffusion inside mucoid biofilms. *Comptes Rendus Biologies*. **328** (12), 1065-1072 (2005).
41. Briandet, R. *et al.* Fluorescence correlation spectroscopy to study diffusion and reaction of bacteriophages inside biofilms. *Applied and Environmental Microbiology*. **74** (7), 2135-2143 (2008).
42. Berney, M., Hammes, F., Bosshard, F., Weilenmann, H. U., Egli, T. Assessment and interpretation of bacterial viability by using the LIVE/DEAD BacLight Kit in combination with flow cytometry. *Applied and Environmental Microbiology*. **73** (10), 3283-3290 (2007).
43. Bergmans, L., Moisiadis, P., Van Meerbeek, B., Quirynen, M., Lambrechts, P. Microscopic observation of bacteria: review highlighting the use of environmental SEM. *International Endodontic Journal*. **38** (11), 775-788 (2005).
44. Hannig, C., Folio, M., Hellwig, E., Al-Ahmad, A. Visualization of adherent micro-organisms using different techniques. *Journal of Medical Microbiology*. **59** (Pt 1), 1-7 (2010).
45. Knutton, S. Electron microscopical methods in adhesion. *Methods in Enzymology*. **253**, 145-158 (1995).
46. Fischer, E. R., Hansen, B. T., Nair, V., Hoyt, F. H., Dorward, D. W. Scanning electron microscopy. *Current Protocols in Microbiology*. **Chapter 2**, Unit 2B.2 (2012).